Dynamic boundary conditions — force

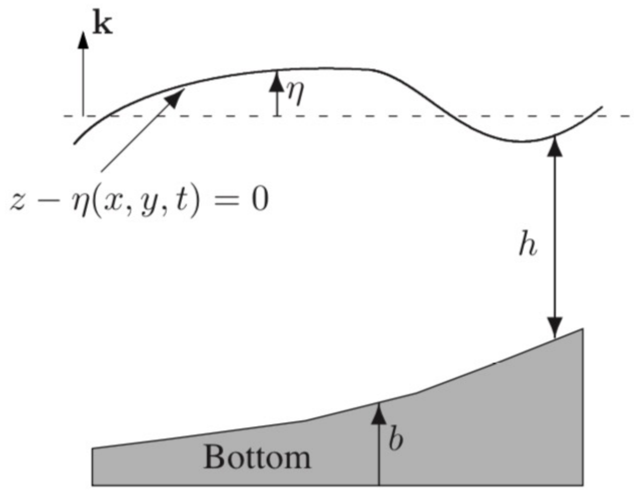

Pressure:

$$p_{\text{atm}} = p_{\text{sea}} \quad \text{at air-sea interface.}$$

$$p_{\text{sea}}(z=0) = p_{\text{atm at sea level}} + \rho_0 g \eta$$

Surface stress:

Stress must be cotinuous along moving boudaries (sea surface)

$$\rho_0 \nu_E \left(\frac{\partial u}{\partial z}\right)\bigg|_{\text{at surface}} = \tau^x, \quad \rho_0 \nu_E \left(\frac{\partial v}{\partial z}\right)\bigg|_{\text{at surface}} = \tau^y$$

The stress must be equal to the wind stress that is parameterized by:

$$U_{10} = \sqrt{u_{10}^2 + v_{10}^2} \qquad \tau^x = C_d\, \rho_{\text{air}}\, U_{10} u_{10}, \quad \tau^y = C_d\, \rho_{\text{air}}\, U_{10} v_{10}$$

Bottom stress:

linear parameterization: $\boldsymbol{\tau} = r_1 \boldsymbol{u}$

quadratic parameterization: $\boldsymbol{\tau} = r_2 |\boldsymbol{u}| \boldsymbol{u}$

logrithmic parameterization: $\boldsymbol{\tau} = \frac{K^2}{ln^2(z/z_0)} |\boldsymbol{u}| \boldsymbol{u}$

K: von Kármán's constant
z_0: roughness length

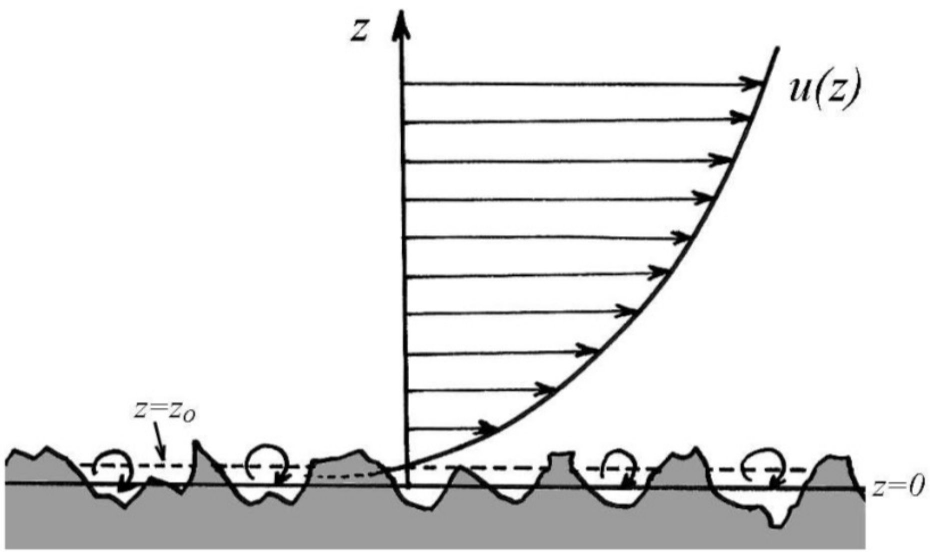

Figure 8-2 Velocity profile in the vicinity of a rough wall. The roughness heigh z_0 is smaller than the averaged height of the surface asperities. So, the velocity u falls to zero somewhere within the asperities, where local flow degenerates into small vortices between the peaks, and the negative values predicted by the logarithmic profile are not physically realized.

Open boundary conditions

Dirichlet condition: Prescribing the value of the variable at the boundary ($\phi = \phi_0$)

Newman condition: setting the gradient to impose the diffusive flux of a quantity ($\kappa \frac{\partial \phi}{\partial n}$)

Cauchy condition: Prescribing a total, advective plus diffusive, flux ($\mathrm{u}\phi - \kappa \frac{\partial \phi}{\partial x}$)

Data source for open boundary conditions**: observations, modelling results**

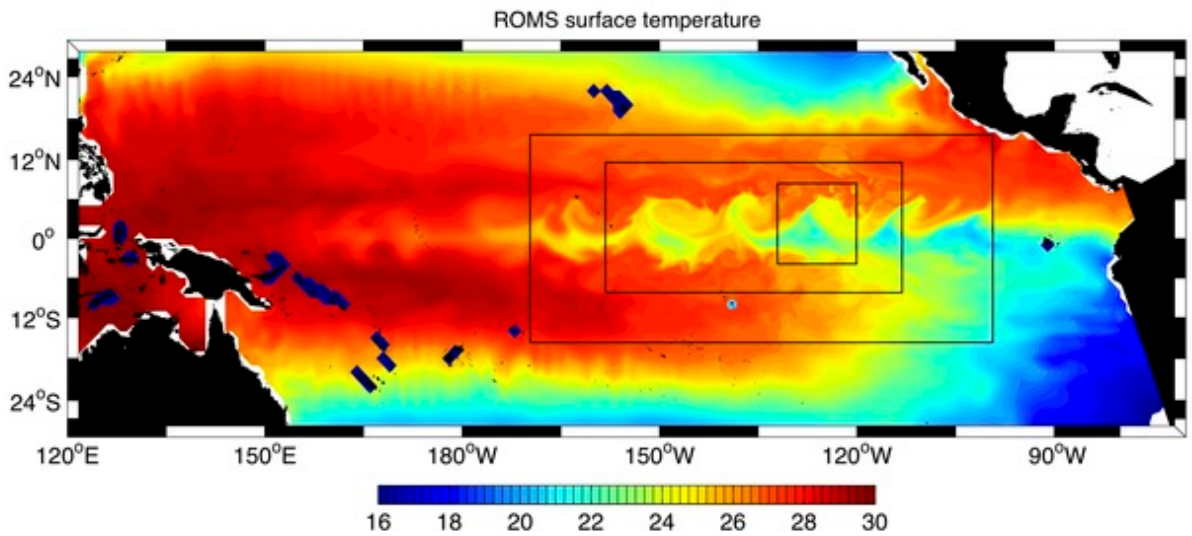

nested models

Part III. Different types of motions

Primitive governing equations

↓ **Assumptions**
(scale analysis, dimensionless numbers)

Simplified governing equations for a motion

↓

Solutions

↓

Characteristics of the motion

Free motions – **Inertial Oscillations**

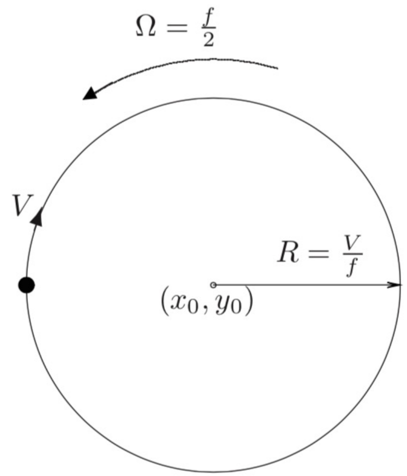

Not subject to real force:

$$\frac{du}{dt} - fv = 0$$

$$\frac{dv}{dt} + fu = 0$$

$$V = \sqrt{u^2 + v^2} \qquad \frac{dx}{dt} \; u = V sin(ft + \phi) \qquad \frac{dy}{dt} \; v = V cos(ft + \phi)$$

f : inertial frequency

$$T = \frac{2\pi}{f}$$

$$x = x_0 - \frac{V}{f}\cos(ft + \phi)$$

$$y = y_0 + \frac{V}{f}\sin(ft + \phi)$$

$$(x - x_0)^2 + (y - y_0)^2 = (\frac{V}{f})^2$$

Table 9.1 Inertial Oscillations

Latitude (φ)	T_i (hr)	D (km) for V = 20 cm/s
90°	11.97	2.7
35°	20.87	4.8
10°	68.93	15.8

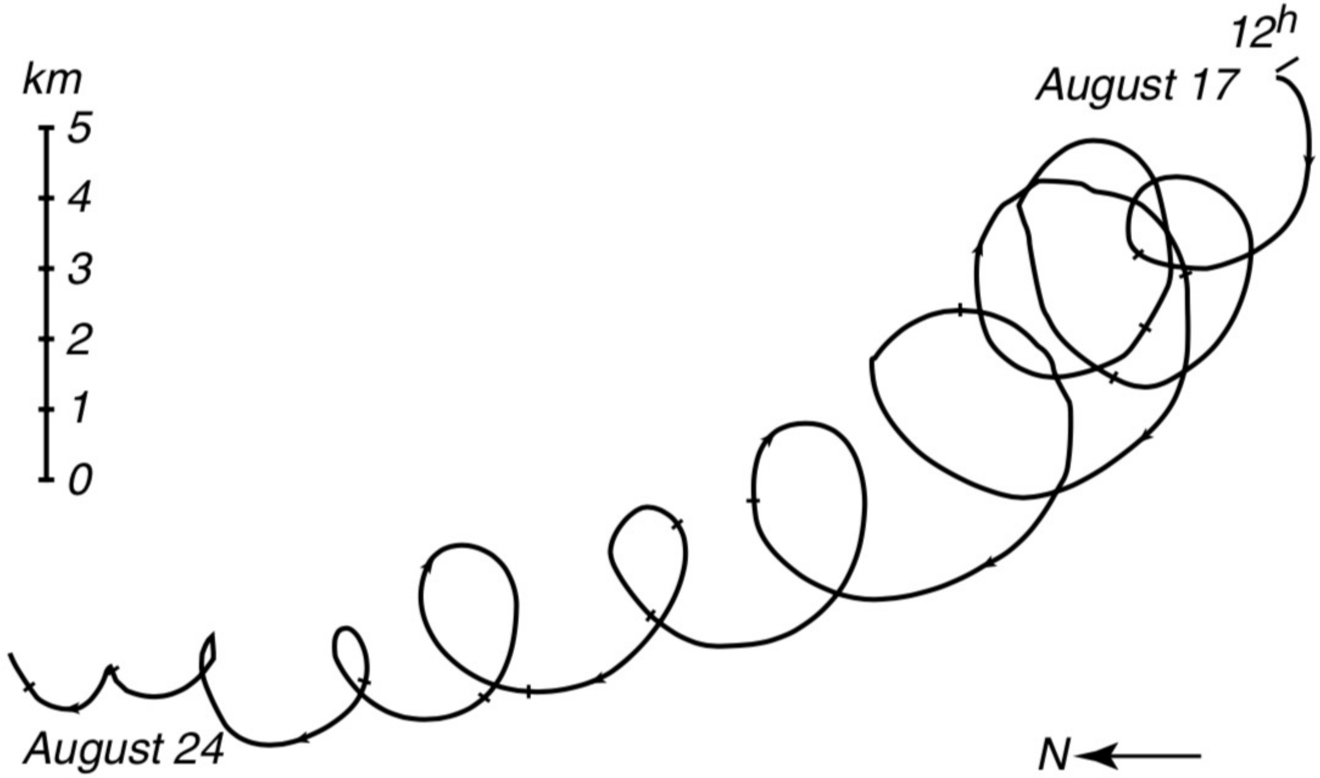

Figure 9.1 Trajectory of a water parcel calculated from current measured from August 17 to August 24, 1933 at 57°49'N and 17°49'E west of Gotland (From Sverdrup, Johnson, and Fleming, 1942).

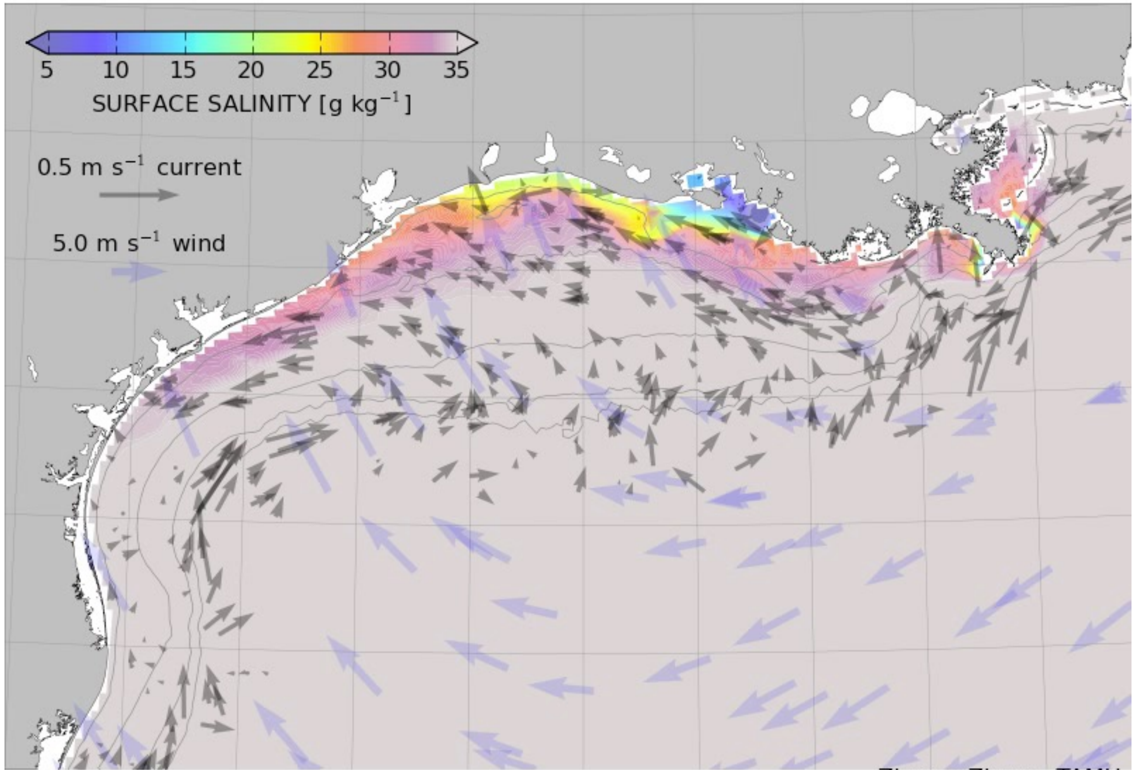

Zhaoru Zhang, TAMU

2006 Feb 28 00:00 GMT

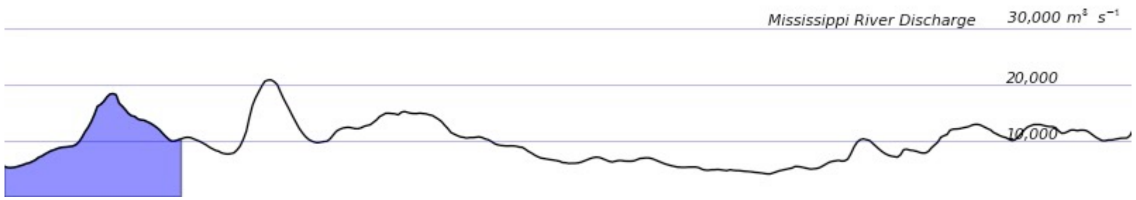

Geostrophic flows

Assumptions:

R_o <<1 and E_k << 1 (ocean interior)

Inertial acceleration, nonlinear advection and viscosity terms are neglected

Governing equations

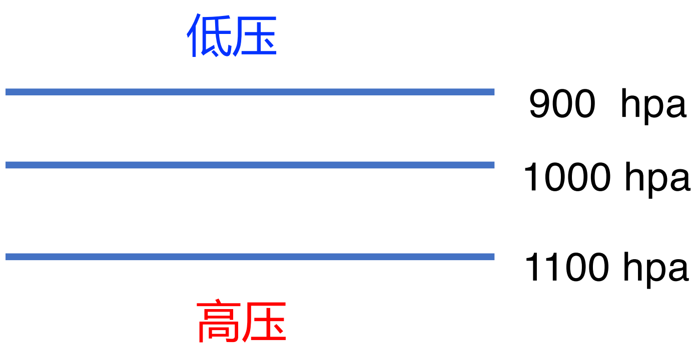

$$\boxed{\begin{aligned} -fv &= -\frac{1}{\rho_0}\frac{\partial p}{\partial x} \\ +fu &= -\frac{1}{\rho_0}\frac{\partial p}{\partial y} \end{aligned}}$$

Geostrophic balance

balance between the pressure gradient term and the Coriolis term

$$\boldsymbol{u} \cdot \nabla p = 0$$

Geostrophic flow is perpendicular to the pressure gradient (force).

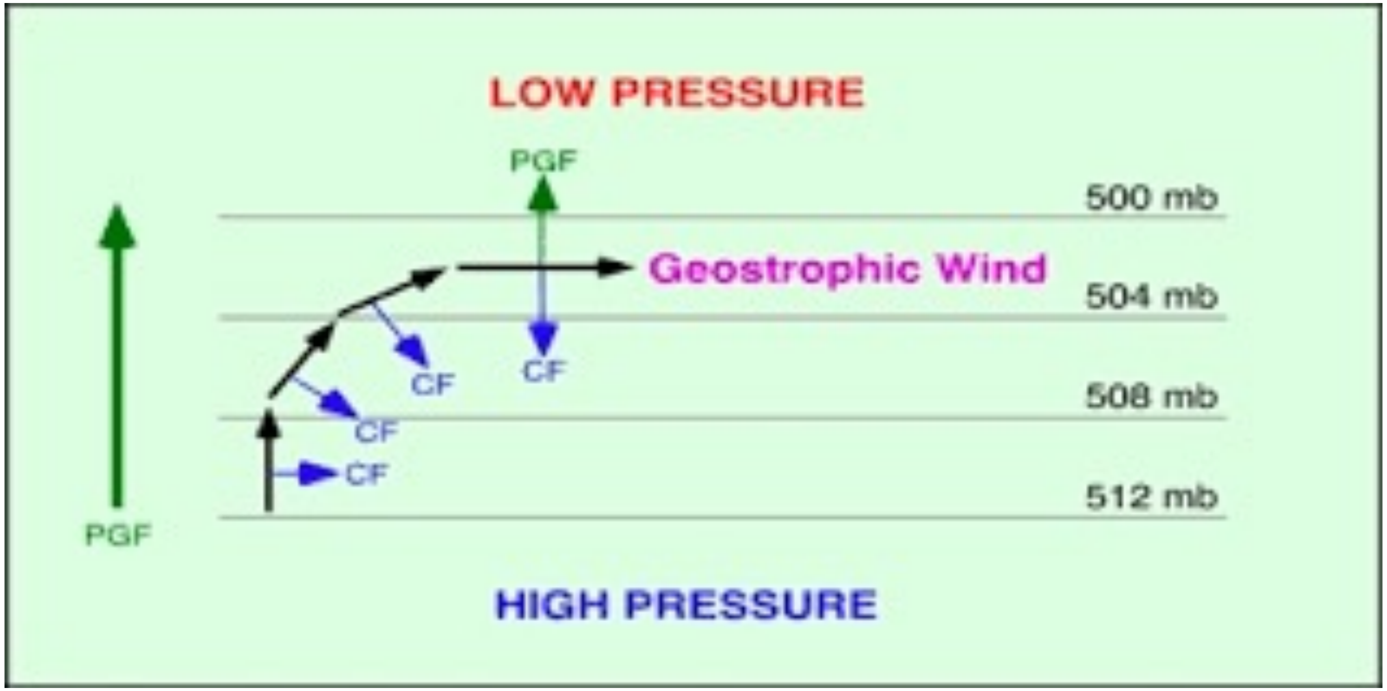

High pressure is to the right (left) of the geostrophic flow in the northern (southern) hemisphere

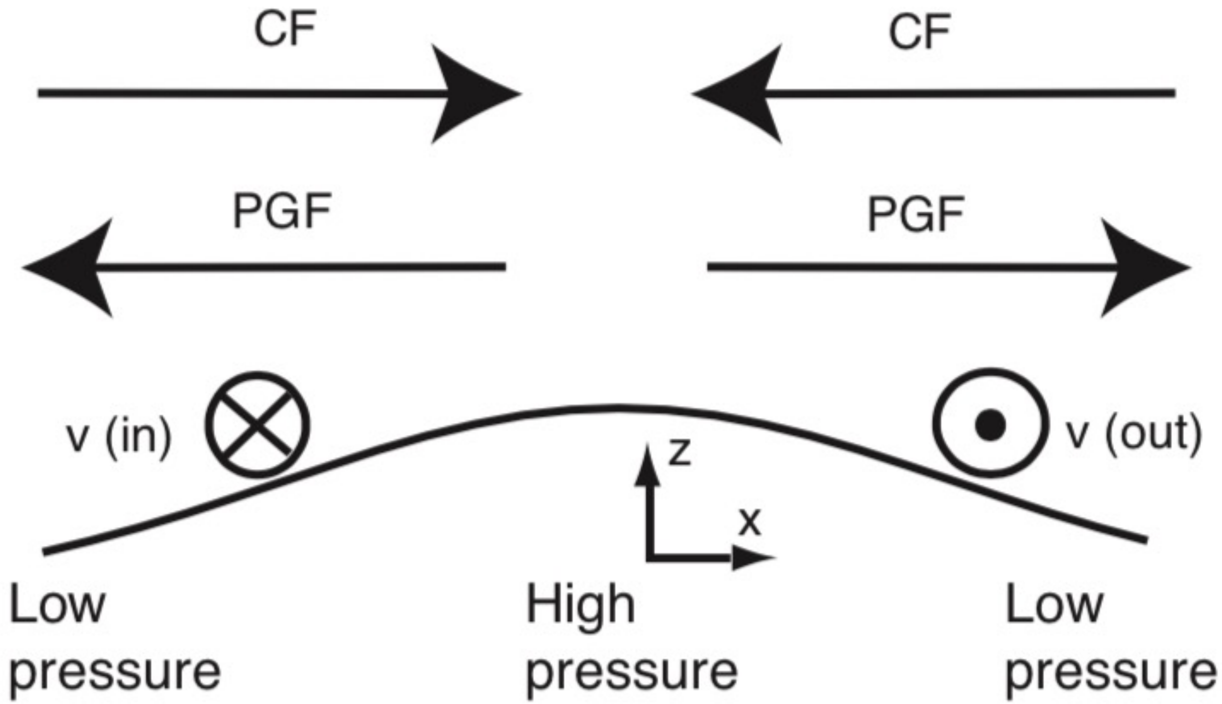

FIGURE 7.9 Geostrophic balance: horizontal forces and velocity. PGF = pressure gradient force. CF = Coriolis force. v = velocity (into and out of page). See also Figure S7.17.

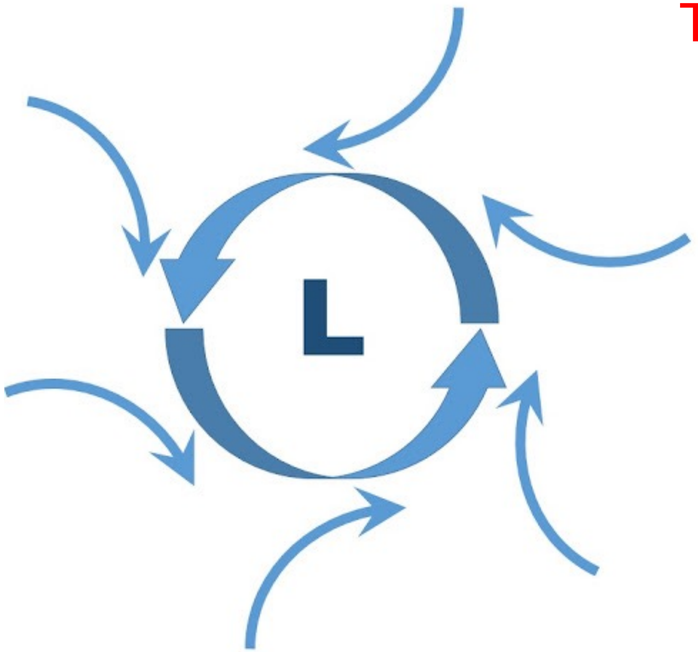

Typhoon：low pressure center

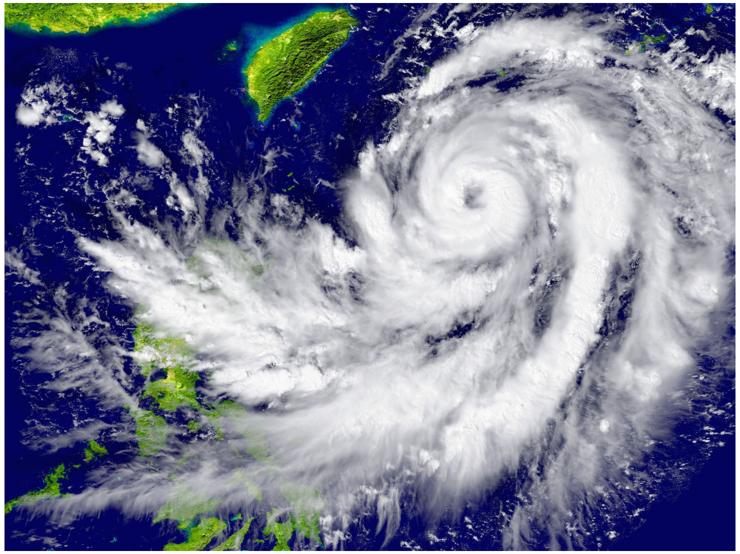

Hurricane

In the northern hemisphere, low-pressure center induces anticlockwise flow (cyclone)

Cyclones and anticyclones

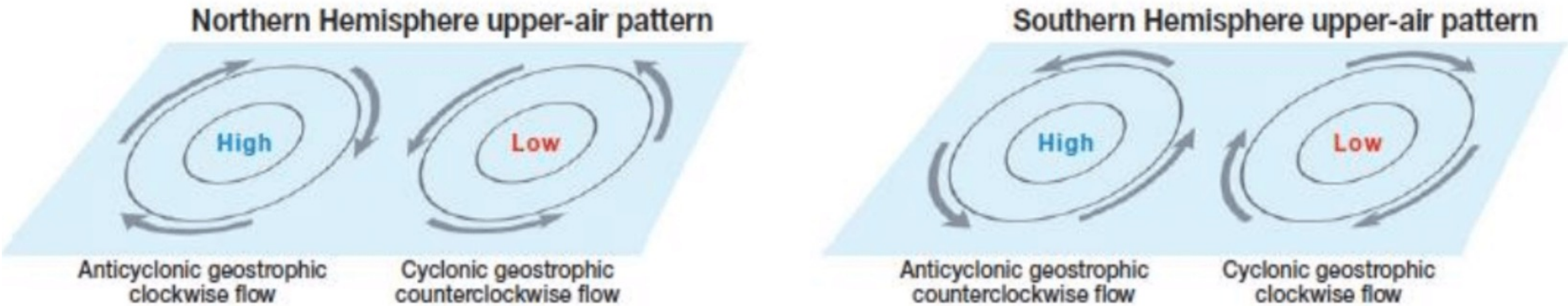

Cyclonic and anticyclonic eddies

northern hemisphere

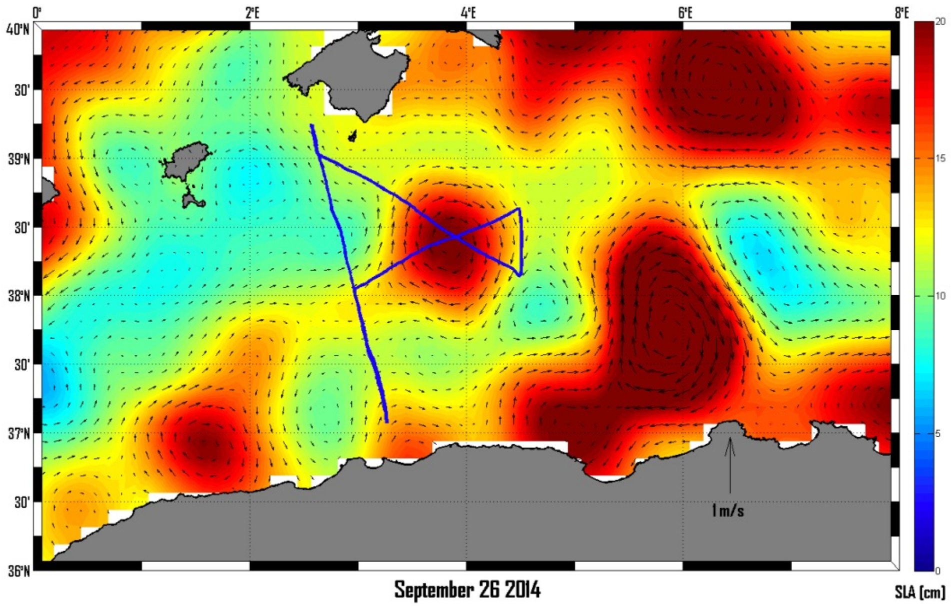

Figure 1: Sea level anomaly map (color scale) and associated geostrophic velocity anomalies (black arrows) from AVISO data on 26 September 2014. Blue line shows the glider track from 15 September to 20 October 2014.

Cotroneo et al. (2015)

southern hemisphere

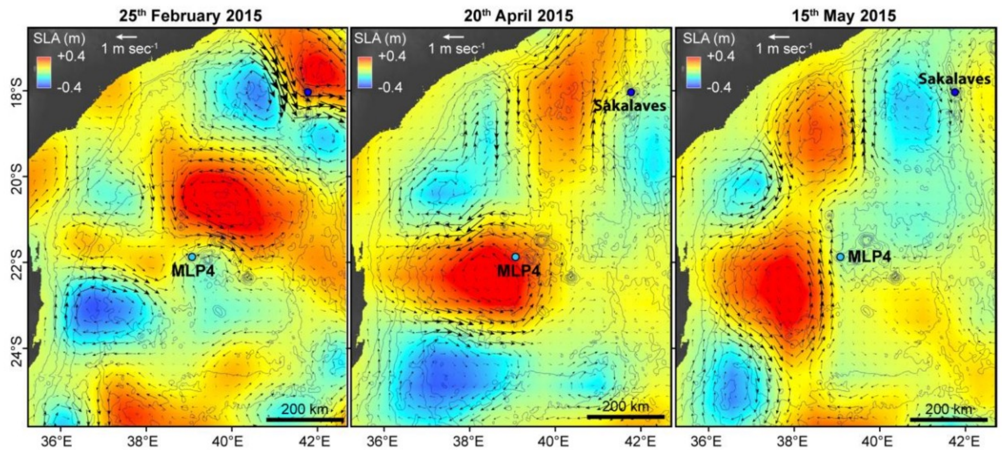

Fig. 16. Sea level anomaly (SLA) and geostrophic velocity anomalies (black arrows) in the Mozambique Channel showing the interaction of large anticyclonic eddies (positive anomalies in red colour) near the seamounts. Bathymetric contours are represented every 500 m.

Miramontes et al. (2018)

Hydrostatic balance $\quad \frac{\partial p}{\partial z} + \rho g = 0$

If $\rho = \rho_0$ everywhere, vertically integrating the equation from z to the surface η :

$$\int_z^\eta \frac{\partial p}{\partial z} dz + \rho_0 g(\eta - z) = 0$$

$$P_o$$

$$p|_z = p|_\eta + \rho_0 g(\eta - z)$$

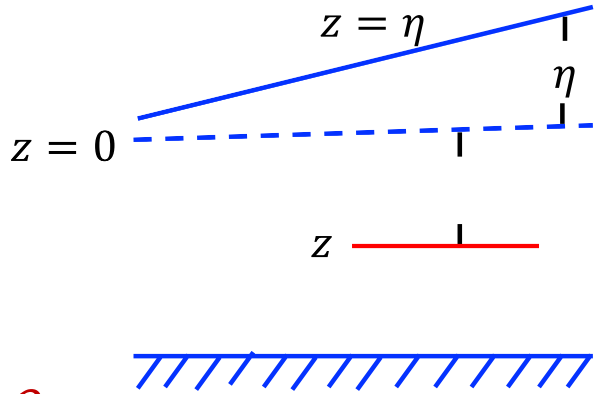

The the horizontal momentum equations become:

$$-fv = -\frac{1}{\rho_0}\frac{\partial}{\partial x}(P_o + \rho_0 g\eta - \rho_0 g\text{z}) = -\text{g}\frac{\partial \eta}{\partial x}$$

$$\text{f}u = -\frac{1}{\rho_0}\frac{\partial}{\partial y}(P_o + \rho_0 g\eta - \rho_0 g\text{z}) = -\text{g}\frac{\partial \eta}{\partial y}$$

So for $\rho = \rho_0$:

$$-fv = -g\frac{\partial \eta}{\partial x}$$

$$fu = -g\frac{\partial \eta}{\partial y}$$

$$\frac{\partial u}{\partial z} = 0$$

$$\frac{\partial v}{\partial z} = 0$$

The flow has no vertical shear and the fluid moves like a slab – **Taylor column**

$$
\boxed{\begin{aligned} -fv &= -\frac{1}{\rho_0}\frac{\partial p}{\partial x} \\ +fu &= -\frac{1}{\rho_0}\frac{\partial p}{\partial y} \end{aligned}}
$$

For f-plane:

$$
\frac{\partial u}{\partial x} + \frac{\partial v}{\partial y} = -\frac{\partial}{\partial x}\left(\frac{1}{\rho_0 f}\frac{\partial p}{\partial y}\right) + \frac{\partial}{\partial y}\left(\frac{1}{\rho_0 f}\frac{\partial p}{\partial x}\right) = 0.
$$

Geostrophic flows are horizontally non-divergent

From the continuity equation: $$\frac{\partial w}{\partial z} = 0$$

For flat surface or bottom, $w = 0$ through the water column

Streamfunction ψ

$$
u = -\frac{\partial \psi}{\partial y}, \qquad v = \frac{\partial \psi}{\partial x}
$$

Geostrophic flow over irregular bottom

Boundary conditions at the surface and bottom:

$$\boxed{\frac{\partial w}{\partial z} = 0}$$

$$w|_{z=\eta} = \frac{\partial \eta}{\partial t} + u\frac{\partial \eta}{\partial x} + v\frac{\partial \eta}{\partial y}$$

$$w|_{z=b} = u\frac{\partial b}{\partial x} + v\frac{\partial b}{\partial y}$$

$$\frac{\partial \eta}{\partial t} + u\frac{\partial \overbrace{(\eta - b)}^{h-H}}{\partial x} + v\frac{\partial \overbrace{(\eta - b)}^{h-H}}{\partial y} = 0$$

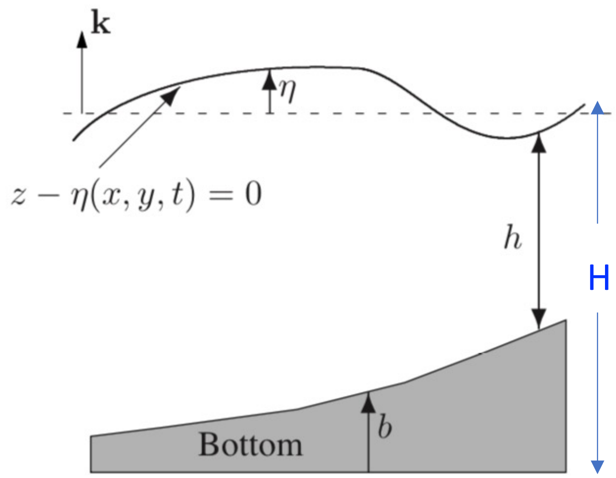

$$\boxed{\eta = h + b - H}$$

For steady motion

$$\boldsymbol{u} \cdot \boldsymbol{\nabla} h = \boldsymbol{0}$$

Geostrophic flows must follow contant h

Geostrophic currents tend to flow along the isobaths

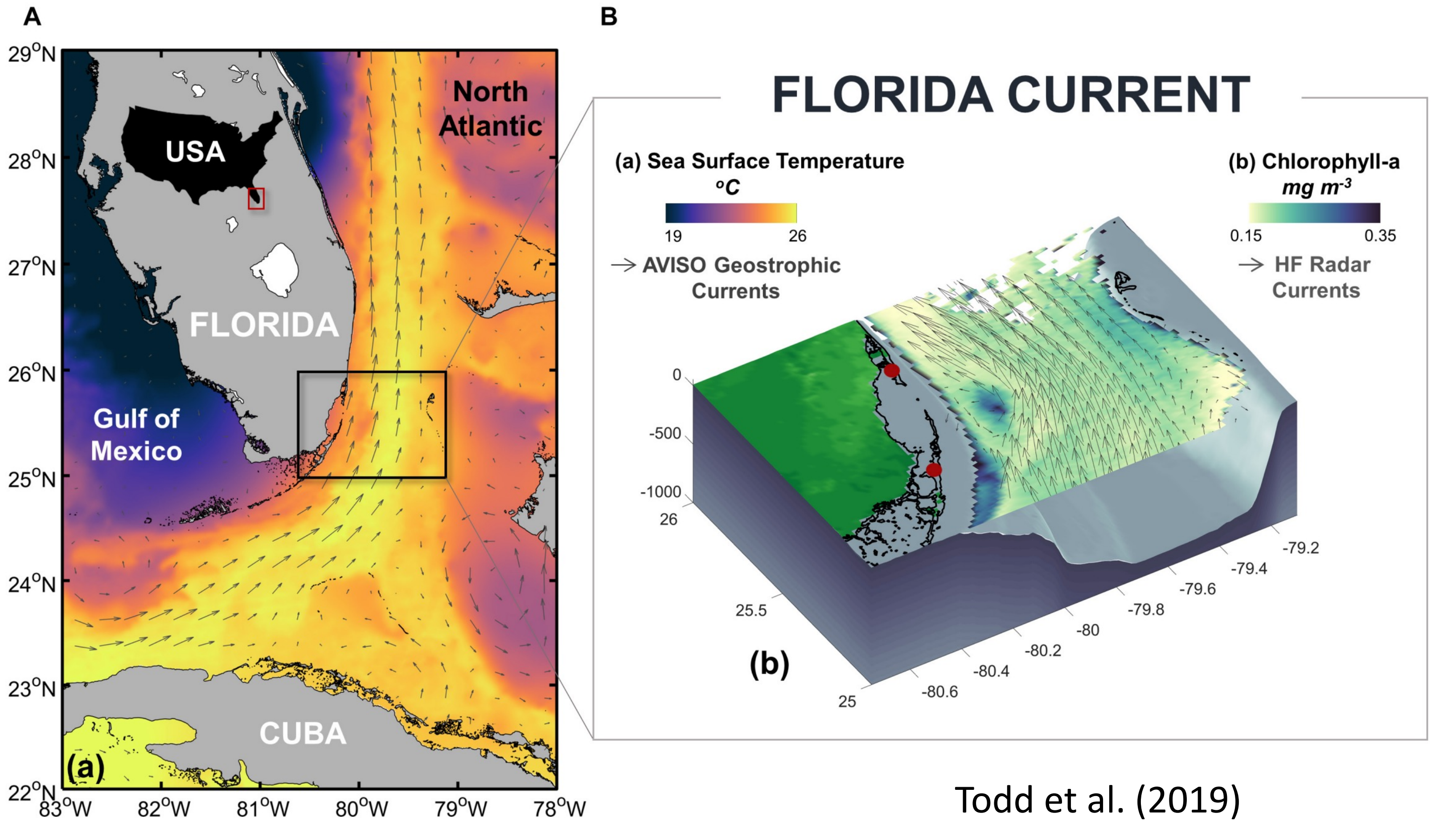

Todd et al. (2019)

FIGURE 4 | Example of combined satellite- and land-based remote sensing of the Florida Current. **(A)** SST from GHRSST and surface geostrophic currents from AVISO. **(B)** Chlorophyll from MODIS AQUA and surface currents from HF radars (HF radar data from Archer et al., 2017b).

Thermal wind balance

$$
\begin{aligned}
-fv &= -\frac{1}{\rho_0}\frac{\partial p}{\partial x} \\
+fu &= -\frac{1}{\rho_0}\frac{\partial p}{\partial y}
\end{aligned}
$$

Hydrostatic balance: $$\frac{\partial p}{\partial z} + \rho g = 0$$

$$
\begin{aligned}
\frac{\partial v}{\partial z} &= -\frac{g}{\rho_0 f}\frac{\partial \rho}{\partial x} \\
\frac{\partial u}{\partial z} &= +\frac{g}{\rho_0 f}\frac{\partial \rho}{\partial y}
\end{aligned}
$$

oceanic front

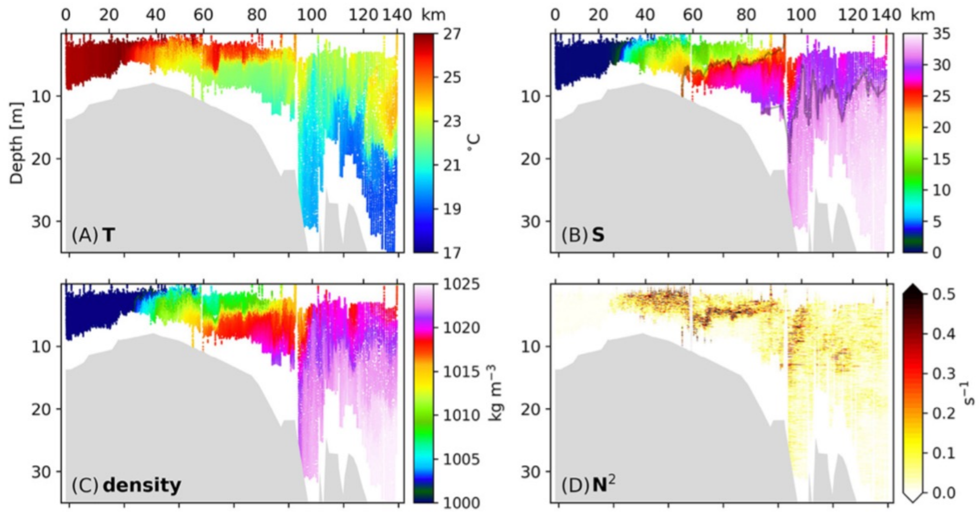

Zhang et al. (2020)

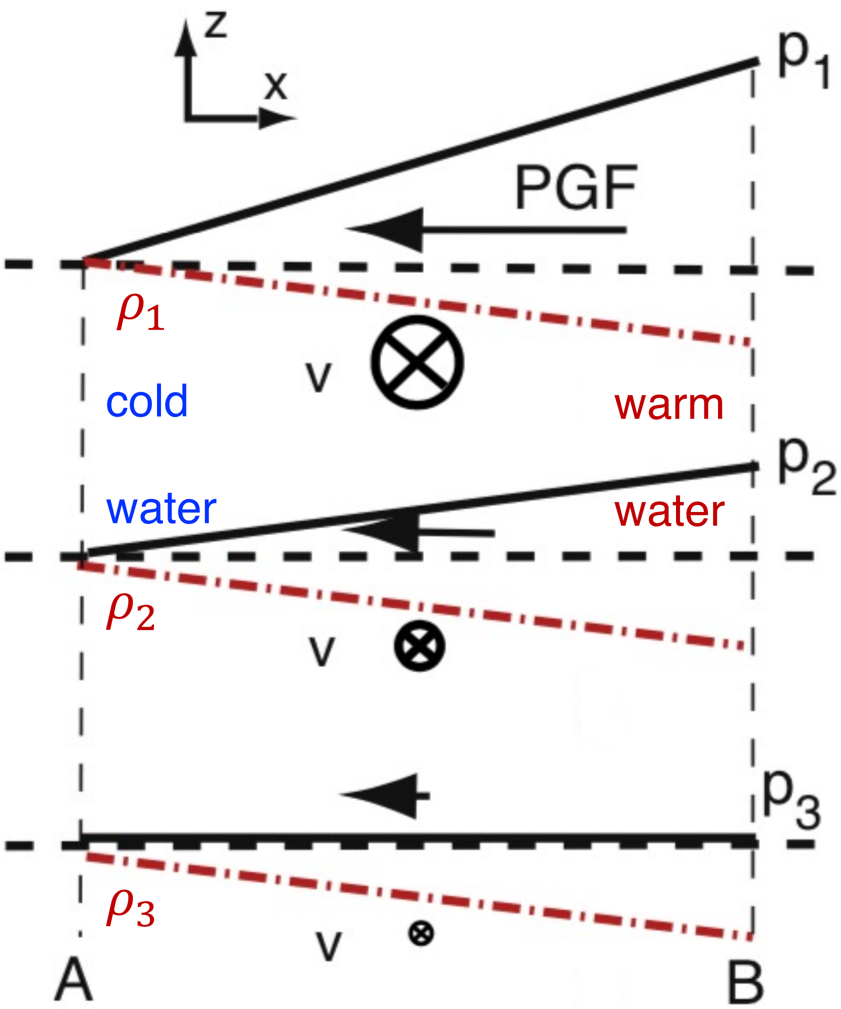

$$-fv = -\frac{1}{\rho_0}\frac{\partial p}{\partial x}$$

$$\frac{\partial v}{\partial z} = -\frac{g}{\rho_0 f}\frac{\partial \rho}{\partial x}$$

FIGURE 7.10 Geostrophic flow and thermal wind balance: schematic of change in pressure gradient force (PGF) with depth. The horizontal geostrophic velocity v is into the page for this direction of PGF and is strongest at the top, weakening with depth, as indicated by the circle sizes. Density (dash-dot) increases with depth, and isopycnals are tilted. With the sea surface at B higher than at A, the PGF at the sea surface (h_1) is to the left. The PGF decreases with increasing depth, as indicated by the flattening of the isobars p_2 and p_3.

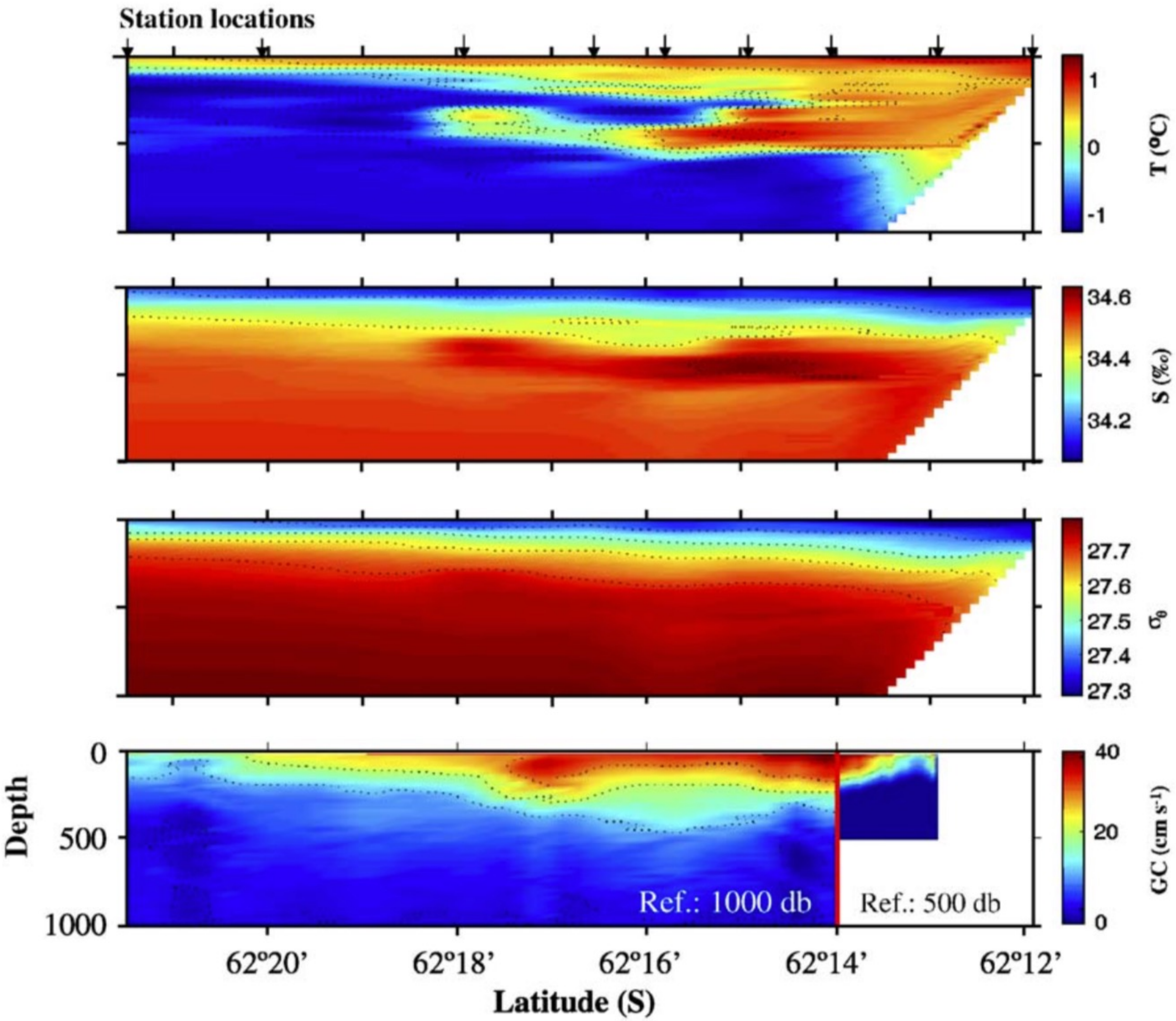

Zhou et al. (2006)

$$\frac{\partial u}{\partial z} = + \frac{g}{\rho_0 f} \frac{\partial \rho}{\partial y}$$

$$\int_{ref}^{z} \frac{\partial u}{\partial z} dz = \frac{g}{\rho_0 f} \int_{ref}^{z} \frac{\partial \rho}{\partial y} dz$$

$$u|_z = \underbrace{u|_{ref}}_{= 0} + \underbrace{\frac{g}{\rho_0 f}}_{f < 0} \overbrace{\int_{ref}^{z} \frac{\partial \rho}{\partial y} dz}^{> 0}$$

Assume at z=1000m (reference depth), $u = 0$

$$\frac{\partial \rho}{\partial y} < 0$$

$u|_z > 0$ (eastward current)

$$\frac{\partial u}{\partial z} > 0$$